



Published in final edited form as:

Hypertension. 2013 August ; 62(2): 310–316. doi:10.1161/HYPERTENSIONAHA.111.00495.

HO-1 Induction Improves Type-1 Cardiorenal Syndrome in Mice with Impaired Ang II-induced Lymphocyte Activation (SCID Mice)

Sumit R. Monu^{1,4}, Paola Pesce^{1,2}, Komal Sodhi^{1,4}, Massimo Boldrin^{1,3}, Nitin Puri⁴, Larisa Fedorova⁴, David Sacerdoti², Stephen J. Peterson⁵, Nader G. Abraham¹, and Attallah Kappas⁶

¹Department of Medicine, Joan C. Edwards School of Medicine, Marshall University, Huntington, WV, 25755, USA

²Department of Medicine, University of Padova, 35100 Padova, Italy

³CORIT-Consortium for Research in Organ Transplantation, University of Padova, 35100 Padova, Italy

⁴Department of Physiology & Pharmacology, University of Toledo College of Medicine, Toledo, OH, 43614, USA

⁵Department of Medicine, New York Medical College, Valhalla, NY, 10595, USA

⁶The Rockefeller University, New York, NY, 10065, USA

Abstract

Type-1 cardiorenal syndrome (CRS-1), characterized by acute kidney dysfunction secondary to cardiac failure and renal arteriolar vasoconstriction, is mediated by the renin-angiotensin-aldosterone axis and sympathetic nervous system activation. Previous reports indicate that AngII modulates immune function and causes recruitment and activation of T lymphocytes. The goal of this study was to evaluate the effects of post-ischemic heart failure on renal morphology and circulation and the beneficial effects of heme oxygenase (HO-1) induction in T-lymphocyte suppressed BALB SCID mice. Mice were divided in 4 groups: sham, myocardial infarction (MI), MI treated with an HO-1 inducer, cobalt protoporphyrin (CoPP), and with or without stannous mesoporphyrin (SnMP), an inhibitor of HO activity. Heart and kidney function were studied 30 days after surgery. Fractional area change was reduced 30 days after surgery in both the C57 and SCID MI-groups as compared to their respective controls ($p < 0.01$). Renal pulsatility index and renal injury were increased in C57 and SCID MI groups compared to the sham group. HO-1 induction improved renal vasoconstriction as well as ameliorated renal injury in both the SCID and C57 MI groups ($p < 0.01$). However, improvement was more evident in SCID mice. In addition, our results showed that plasma creatinine, Ang II and renin were significantly increased in the C57 and SCID MI groups as compared to their respective controls. HO-1 induction decreased these parameters in both MI groups. SnMP reversed the beneficial effect of CoPP in both mouse strains. The study demonstrates that T-lymphocyte suppression facilitated the HO-1 dependent improvement in the attenuation of CRS-1.

Corresponding author: Nader G. Abraham, PhD., Dr. H.C., FAHA, Professor, Marshall University Joan Edwards School of Medicine, Huntington, West Virginia, 25701-3655, FAX: 304 691-1726, Tel 304-691-1791, abrahamn@marshall.edu.

Conflicts of Interest and Disclosures: None.

Publisher's Disclaimer: This is a PDF file of an unedited manuscript that has been accepted for publication. As a service to our customers we are providing this early version of the manuscript. The manuscript will undergo copyediting, typesetting, and review of the resulting proof before it is published in its final citable form. Please note that during the production process errors may be discovered which could affect the content, and all legal disclaimers that apply to the journal pertain.

Keywords

heart failure; renal vasoconstriction; T-lymphocytes; ANGII; HO-1

Introduction

Type 1 cardiorenal syndrome (CRS-1) is characterized by acute kidney dysfunction secondary to decompensated heart failure. Several pathophysiological mechanisms have been proposed to explain the interaction between heart and kidney during heart failure^{1,2}. A model based on 4 interrelated cardiorenal connectors: the renin angiotensin aldosterone system (RAAS), the sympathetic nervous system (SNS), inflammation and nitric oxide (NO)/reactive oxygen species (ROS) balance has been proposed. Ang II and SNS activation induce renal vasoconstriction³ which can be noninvasively evaluated by renal Doppler sonography⁴. The interaction between oxidative stress, inflammation and activation of RAS has been well documented^{5,6}.

Ang II increases in heart failure in an attempt to balance the hypoperfusion of the kidney due to decreased cardiac output. In addition Ang II plays a key role in the development of cardiorenal syndrome because of its association with increased vascular ROS production in kidney, which contributes to renal injury⁷. Various experimental models of excess Ang II demonstrate myocardial and renal fibrosis secondary to increased inflammation^{8,9}. Recent studies on the role of Ang II and aldosterone in the pathogenesis of hypertension have shown that both compounds initiate vascular and tissue inflammation that leads to the activation of the immune response¹⁰. More specifically, the accumulation of T-cells in the vasculature appears to play a critical role in the development of hypertension. Reports have also shown that Ang II induced recruitment of T-lymphocytes in renal cortical interstitium aggravates renal damage¹¹.

Heme oxygenase-1 (HO-1) is a cytoprotective enzyme that degrades heme (a pro-oxidant) to generate carbon monoxide (CO, a vasodilatory gas that also has anti-inflammatory properties), bilirubin (an antioxidant derived from biliverdin), and iron⁷. HO-1 is present in heart and renal tissue¹² and low levels lead to cardiac and renal dysfunction¹³⁻¹⁶. Upregulation of HO-1 has a cardio- and reno-protective function mediated by its anti-oxidative, anti-inflammatory and anti-apoptotic properties¹⁷⁻¹⁹.

In animal models of myocardial ischemia (MI), both over-expression and pharmacological induction of HO-1 reduce infarct size and ventricular remodeling after ischemia reperfusion damage, by improving cardiac metabolism^{15,20,21}. Increased HO-1 expression has a protective effect against ischemia reperfusion injury in the kidney, and can correct blood pressure elevation following Ang II exposure¹⁵. The therapeutic effect of HO-1 induction during cardiac ischemic damage has been studied but little is known about the beneficial effects of increased levels of HO-1 4 weeks after MI at 4 weeks and the role of the enzyme in limiting CRS-1. CO reduces renal arteriolar vascular tone by its effect on BCa channels, and decreases phenylephrine induced vasoconstriction in mesenteric vessels^{22,23}. In addition, increased levels of HO-1 counteract aldosterone-elicited arterial injury through the inhibition of both oxidative stress and inflammation⁷. HO-1 interacts with T-lymphocyte mediated immunity, playing an immunosuppressive role²⁴⁻²⁶. Thus HO-1 induction could be considered as a therapeutic approach to the treatment of CRS-1.

This study demonstrates the role of T-lymphocytes in CRS-1 and the beneficial effects of HO-1 induction in attenuating cardiorenal syndrome in immuno-competent and immuno-suppressed mice after post ischemic heart failure.

Materials and Methods

The animal protocols were approved by the University of Toledo Animal Care and Use Committee and performed according to the Guide for the Care and Use of Laboratory Animals published by the National Institutes of Health (NIH Publication No. 85-23, revised 1996).

Twenty-five SCID and 19 C57 male mice weighing 22-26g, aged 8 to 10 weeks, were purchased from Jackson Laboratories (Bar Harbor, ME). Mice were housed under SPF conditions, in a single ventilated cage system, fed standard mouse pellets and water *ad libitum*.

Design of the study

Both animal models i.e. C57 as well as SCID mice were divided in 4 groups: - Control, MI, MI treated with CoPP and MI treated with CoPP and SnMP.

Left anterior descending coronary artery ligation (LAD) method

Animals were anesthetized using ketamine and xylazine (80 mg/Kg and 10 mg/Kg respectively). Animal chests were shaved and intubation was done by the endotracheal method. After intubation animals were kept on ventilation with 100% oxygen and isoflurane (0.75% to 1.5%) at 180 breaths per minute using a MiniVent Mouse Ventilator (type 845, Harvard Apparatus). Body temperature was maintained at 37°C by using a Heating pad. Left thoracotomy was performed in the 3rd intercostal space under sterile conditions and the pericardium was opened to expose the heart. An 8.0 prolene ligature (Ethicon) was tied around the proximal left coronary artery, just distal to the left atrial appendage border. Blanching of the anterolateral region of the left ventricle (LV) was used to confirm infarction. Chest was then closed with a single 5.0 silk suture between the 3rd and 4th ribs and muscle layers were recomposed. After closing the skin with a continuous suture, all mice were hydrated with saline and were given an analgesic, carprofen at the dose of 4 mg/Kg, for two days. At the end of the surgery mice were housed for 24 hours in an incubator at 37°C and then allowed to recover in single cages and monitored twice a day for 7 days. Control surgery was performed without coronary artery ligation. All groups underwent echocardiography and renal echoDoppler examination 30 days after surgery.

Echocardiographic evaluation—Transthoracic echocardiography was performed using a Siemens Acuson Sequoia sonography machine with a 15 MHz linear probe. Animal chests were shaved. Animals were anesthetized with 3% isoflurane and temperature controlled anesthesia was maintained with 1.5% isoflurane. Two-dimensional cine loops and M-mode cine loops of a long-axis view and a short-axis view of the LV were recorded. All mice were imaged by a single operator.

End-diastolic and end-systolic areas (EDA, ESA), end-diastolic and end-systolic length (EDL, ESL) were measured from the long axis B-mode image and end-diastolic and end-systolic diameter (EDD, ESD) were measured from the short axis M-mode image. Fractional Area Change (FAC), an index of LV contractile function, was determined using the following formula: $FAC = (EDA - ESA) / EDA$. Aortic Doppler flow was measured from B-mode images of a long axis view, placing the sample volume at the level of the aortic efflux tract. Aortic velocity –time integral (Ao VTI) was measured from aortic Doppler-flow curve. Aortic outflow tract diameter (Ao OFT) was measured from the same B-mode images of a long axis view.

Stroke volume (S.V.) was calculated using the following formula:

Stroke volume = $3.14 \times (\text{Aortic outflow tract diameter}/2)^2 \times \text{Aortic velocity} \times \text{time interval}$

Cardiac index (C.I.) was calculated using the following formula:

$$\text{Cardiac index} = (\text{Stroke volume} \times \text{heart rate}) / \text{Body weight.}$$

Renal echoDoppler evaluation—Immediately after echocardiographic evaluation renal echoDoppler was performed using the same probe (Siemens Acuson Sequoia echo machine with a 15 MHz linear probe). Abdomens of the mice were shaved and Doppler analysis of interlobar arteries blood flow was performed from a transversal B-mode image of both kidneys placing the sample volume in the renal cortex. All mice were imaged by a single operator. Peak Velocity (Vmax), End Diastolic Velocity (Vmin) and Mean Velocity (VM) were measured and Pulsatility Index (K-PI) was determined using the following formula

$$\text{Renal pulsatility index} = (\text{Peak velocity} - \text{End diastolic velocity}) / (\text{Mean velocity})$$

4.

Renal Histology

Formalin-fixed, paraffin-embedded kidney sections were cut 5 μm thick, deparaffinized and rehydrated. For collagen detection, slides were incubated in saturated picric acid containing 0.1% of Direct Red (Sigma) for 1 hour in the dark. Images were captured on a Nikon Eclipse 80i microscope equipped with a Nikon camera head DS-Fi1 (Niko, Tokyo, Japan). For quantitative analysis at least 4 randomly chosen fields from each animal were digitized. Collagen volume was determined using the Image J software (<http://rsbweb.nih.gov/ij>)²⁷.

Plasma Renin and Angiotensin II levels

The plasma levels of Renin and Angiotensin II level were measured in plasma using an ELISA assay (Assay Gate, Inc. Ijamsville, MD). Briefly, the angiotensin II measurements are based on the competitive method of enzyme linked immunoassays. The antiserum is captured by antibodies coated on a 96-well plate. The angiotensin II concentration in the sample is determined directly from the standard curve. The mouse renin immunoassay is based on a solid phase sandwich enzyme linked immunoassay (ELISA) method. Samples, calibrators and controls are added to the wells coated with monoclonal antibody to mouse Renin. After incubation step, the mouse renin binds to the monoclonal antibody on the well. A standard curve is prepared relating color intensity to the concentration of renin on each plate. Positive and negative controls on a plate are used. The tests are end-point measurements and in duplicates.

Plasma Creatinine levels

Plasma Creatinine levels were measured by an enzyme-linked immunoassay (Cayman Chemical Co., Ann Arbor, MI) according to the manufacturer's instructions²⁸.

Drug administration

Cobalt Protoporphyrin administration: Cobalt Protoporphyrin (CoPP), a potent HO-1 inducer, was administered via intraperitoneal injection 5 days after LAD ligation and then every 5 days for 4 weeks at a dose of 3 mg/Kg body weight.

Tin Mesoporphyrin administration: Tin Mesoporphyrin (SnMP), an inhibitor of HO activity, was administered at a dose of 20 mg/Kg body weight via intraperitoneal injection every 2 days for 15 days before euthanasia.

Statistical Analysis

Data are expressed as means \pm S.E.M. Significance of difference in mean values was determined using one-way analysis of variance followed by the Newman-Keul's post hoc test. $P < 0.05$ was considered to be significant.

Results

Body weight measurement

Mice were examined 30 days after MI and their body weights were not significantly different in any of the treated groups of both C57 and SCID animals when compared with sham operated controls (Table 1).

Echocardiographic examination

Thirty days after MI EDA and EDD were increased in both C57 and SCID mice when compared to sham operated control ($p < 0.01$ respectively). CoPP treatment reduced both EDA and EDD to sham operated levels (Table 1). EDA was reduced significantly ($p < 0.05$) in both C57 and SCID when compared to MI mice. A similar result was seen with EDD, a ($p < 0.01$) decrease was seen in C57 mice and a ($p < 0.05$) decrease in SCID mice when compared with MI mice. SnMP abolished the effects of CoPP and the values of EDA and EDD were similar to those in the MI mice (Table 1). 30 days after MI, C.I. was significantly reduced in both C57 and SCID mice because of reduced LV systolic function (Table 1). Administration of CoPP improved C.I. compared to the MI group in both C57 and SCID mice. Concurrent administration of SnMP reversed the beneficial effects of CoPP. MI resulted in a significant decrease in FAC in both C57 ($p < 0.05$) and SCID ($p < 0.01$) mice when compared to sham operated animals. CoPP restored FAC levels to those of the sham operated animals. SnMP reversed the effects of CoPP (Figure 1).

Renal echoDoppler examination

Renal arterial resistance indices were significantly lower in SCID mice than in C57 mice (Fig. 2). Both C57 and SCID mice developed significant renal vasoconstriction 30 days after MI (Fig. 2). In CoPP treated C57 and SCID mice, K-PI decreased in comparison to the MI group (Fig. 2C). However, the reduction was more pronounced in SCID mice administered CoPP (30% reduction in SCID mice vs. 18% decrease in C57 mice in renal vasoconstriction Fig. 2 D, $p < 0.05$). Concurrent administration of SnMP with CoPP increased renal vasoconstriction in both C57 and SCID MI mice treated with CoPP (Fig. 2C and D).

Renal Histology examination

Collagen I & III staining of both C57 and SCID kidney tissue revealed the presence of perivascular and peritubular interstitial fibrosis at the corticomedullary junction. Fibrosis was higher in MI groups in both C57 and SCID mice as compared to control mice (Fig. 3A and Fig. 3B). However, the level of collagen accumulation in SCID MI mice was significantly lower than C57 MI mice ($p < 0.02$). CoPP reduced renal fibrosis in both SCID and C57 mice as compared to the MI group, the effect being more evident in SCID mice (Fig. 3A and Fig. 3B). Concurrent administration of SnMP reversed the beneficial effects of CoPP (Fig. 3A and Fig. 3B).

Plasma Creatinine levels

As seen in Fig. 4A and Fig. 4B, plasma creatinine was significantly higher in the MI group of both C57 and SCID mice ($p < 0.05$). However, the plasma creatinine level in SCID MI mice was significantly lower than in C57 MI mice ($p < 0.05$). CoPP significantly decreased plasma creatinine levels in both C57 and SCID mice, the effect being more evident in SCID mice (26% reduction in plasma creatinine levels compared to 17% reduction in C57 mice), and this effect was reversed by the concurrent administration of SnMP in both C57 and SCID mice ($p < 0.05$) (Fig. 4C and 4D).

Plasma Renin and Angiotensin II levels

Myocardial infarction is accompanied by the activation of the RAS system and was examined by the measurement of plasma renin and angiotensin II levels. Plasma renin (Fig. SA and Fig. SB respectively) and angiotensin II levels (Fig. SC and Fig. SD respectively) were significantly higher in C57 and SCID MI groups as compared to their respective control groups ($p < 0.05$). CoPP significantly decreased these RAS markers in both strains and this beneficial effect of HO-1 induction was reversed by concurrent administration of SnMP ($p < 0.05$) (Figs. SA, SB, SC and SD).

Discussion

This study demonstrates for the first time the beneficial effects of HO-1 induction in improving CRS-1 in immuno-competent and immuno-suppressed mice. We demonstrate that Ang II mediated recruitment of T lymphocytes and increased oxidative stress is decreased by the upregulation of HO-1 in a model of post ischemic heart failure. Our results show that HO-1 induction decreased renal vasoconstriction and fibrosis and improved renal function in both immuno-competent and T lymphocyte suppressed mice, the effect being more prominent in the latter SCID mice.

Thirty days after left anterior descending coronary ligation, C57 and SCID mice developed heart failure characterized by a significant dilatation of the left ventricle with a reduction in FAC. A reduction in FAC leads to a functional hypovolemia and the activation of SNS and RAAS, and the release of an anti-diuretic hormone²⁹. CoPP improved cardiac function, as evidenced by increased FAC and decreased EDA in both SCID and C57 mice. Previous reports have shown that Ang II modulates immune function and causes T lymphocyte activation and proliferation¹¹ Attributing a role of T-lymphocytes in hypertension³⁰; we expected that SCID mice would be resistant to the development of CRS-1. As expected, SCID mice had lower basal renal arterial resistance in comparison to the C57 mice probably due to the absence of T-lymphocyte-Ang II interaction. In the MI group, both mouse strains exhibited a significant increase in renal arterial resistance which was attenuated by the upregulation of HO-1. The CoPP mediated improvement was more evident in SCID mice suggesting the role of T-lymphocytes in CRS-1. Our findings are in agreement with previous reports showing that T-lymphocytes play an important role in hypertension³¹. Thus it appears that renal vasoconstriction is not related strictly to heart failure but is influenced by other mechanisms that involve interactions between HO-1, RAAS and T-lymphocytes.

The role of RAS well established in the initiation and maintenance of vascular, myocardial and renal dysfunction in CRS-1³². Consistent with these reports, Ang II and renin levels were increased in the circulation in both C57 and SCID MI groups and were decreased by CoPP.

One of the pathological abnormalities observed in CRS-1 is renal damage manifest by increased plasma creatinine levels³³. Our results demonstrate that C57 and SCID MI groups have not only altered metabolic homeostasis but also increased renal damage, as evidenced

by increased collagen deposition and the deterioration in renal function. The production of inflammatory cytokines, due to ischemic cardiac damage, causes a systemic inflammatory activation in which the kidney is involved. Systemic inflammation, together with Ang II activation, results in T-lymphocyte recruitment³¹ and further renal damage³⁴. Activated T-lymphocytes amplify the Ang II effect stimulating vascular ROS production in kidney contributing to a further increase in ROS and added renal damage and dysfunction^{5,35}. Consistent with these reports, we show that plasma creatinine levels and renal damage was less in T lymphocyte suppressed mice (SCID) when compared to C57 mice due to the absence of a T-lymphocyte-RAS interaction. Thus, T lymphocytes contribute to the pathological effects of RAS dysregulation in CRS-1. HO-1 induction is associated with a decrease in T lymphocyte proliferation (7393). Our results demonstrate that the beneficial effects of increased levels of HO-1 in improving CRS-1 are more apparent in SCID mice than in C57 mice, suggesting that the decrease of the T lymphocyte immune response amplified the effects of HO-1 in attenuating CRS-1. SnMP reduced the beneficial effects of HO-1 induction on left ventricle contractile function (FAC) and dilatation (EDA, EDD) in C57 and SCID mice and caused a deterioration in renal vasoconstriction and renal function. The fact that SnMP reversed the beneficial effects of CoPP is a clear indication that increased levels of HO activity plays a central role in preventing MI- induced cardiac and renal damage in this animal model. These observations offer a portal in the development of therapeutic approaches to prevent the irreversible damage that occurs after MI.

In conclusion (scheme 6), we demonstrate that a decrease of the T-Lymphocyte immune response reduces kidney damage and renal vasoconstriction in a model of post ischemic heart failure, and that suppression of T lymphocytes amplified the beneficial effects of HO-1 in improving CRS-1.

Perspectives

We show that T-lymphocyte suppression facilitated the HO-1 dependent improvement in attenuating CRS-1 after post ischemic heart failure. This is of clinical benefit as it highlights potential approaches to reverse the detrimental cardiac and renal perturbations associated with MI by pharmacological induction of HO-1.

Supplementary Material

Refer to Web version on PubMed Central for supplementary material.

Acknowledgments

All authors had full access to the data and take responsibility for its integrity. All authors have read and agree with the manuscript as written.

Source of Funding: This work was supported by National Institutes of Health grants DK56601(NGA), HL-34300 (NGA) and BrickStreet Foundation Inc. (NGA) and gifts from the Renfield Foundation to The Rockefeller University (AK).

References

1. Bongartz LG, Cramer MJ, Braam B. The cardiorenal connection. *Hypertension*. 2004; 43:e14. [PubMed: 14967846]
2. Bongartz LG, Cramer MJ, Doevendans PA, Joles JA, Braam B. The severe cardiorenal syndrome: 'Guyton revisited'. *Eur Heart J*. 2005; 26:11–17. [PubMed: 15615794]
3. Badzynska B, Sadowski J. Moderate intrarenal vasoconstriction after high pressor doses of norepinephrine in the rat: comparison with effects of angiotensin II. *Kidney Blood Press Res*. 2011; 34:307–310. [PubMed: 21606652]

4. Sacerdoti D, Bolognesi M, Merkel C, Angeli P, Gatta A. Renal vasoconstriction in cirrhosis evaluated by duplex Doppler ultrasonography. *Hepatology*. 1993; 17:219–224. [PubMed: 8428719]
5. De MC, Das S, Lund H, Mattson DL. T lymphocytes mediate hypertension and kidney damage in Dahl salt-sensitive rats. *Am J Physiol Regul Integr Comp Physiol*. 2010; 298:R1136–R1142. [PubMed: 20147611]
6. Zablocki D, Sadoshima J. Angiotensin II and Oxidative Stress in the Failing Heart. *Antioxid Redox Signal*. 2012 In Press.
7. Abraham NG, Kappas A. Heme oxygenase and the cardiovascular-renal system. *Free Radic Biol Med*. 2005; 39:1–25. [PubMed: 15925276]
8. Marvar PJ, Thabet SR, Guzik TJ, Lob HE, McCann LA, Weyand C, Gordon FJ, Harrison DG. Central and peripheral mechanisms of T-lymphocyte activation and vascular inflammation produced by angiotensin II-induced hypertension. *Circ Res*. 2010; 107:263–270. [PubMed: 20558826]
9. Chu PY, Zatta A, Kiriazis H, Chin-Dusting J, Du XJ, Marshall T, Kaye DM. CXCR4 antagonism attenuates the cardiorenal consequences of mineralocorticoid excess. *Circ Heart Fail*. 2011; 4:651–658. [PubMed: 21685249]
10. Kasal DA, Schiffrin EL. Angiotensin II, Aldosterone, and Anti-Inflammatory Lymphocytes: Interplay and Therapeutic Opportunities. *Int J Hypertens*. 2012; 2012:829786. [PubMed: 22685633]
11. Suzuki Y, Ruiz-Ortega M, Gomez-Guerrero C, Tomino Y, Egido J. Angiotensin II, the immune system and renal diseases: another road for RAS? *Nephrol Dial Transplant*. 2003; 18:1423–1426. [PubMed: 12897073]
12. Abraham NG, Pinto A, Levere RD, Mullane K. Identification of heme oxygenase and cytochrome P-450 in the rabbit heart. *J Mol Cell Cardiol*. 1987; 19:73–81. [PubMed: 3550106]
13. Abraham NG, Kappas A. Mechanism of heme-heme oxygenase system impairment of endothelium contraction in the spontaneously hypertensive rat. *Hypertension*. 2011; 58:772–773. [PubMed: 21947469]
14. Perrella MA, Yet SF. Role of heme oxygenase-1 in cardiovascular function. *Curr Pharm Des*. 2003; 9:2479–2487. [PubMed: 14529547]
15. Yet SF, Tian R, Layne MD, Wang ZY, Maemura K, Solovyeva M, Ith B, Melo LG, Zhang L, Ingwall JS, Dzau VJ, Lee ME, Perrella MA. Cardiac-specific expression of heme oxygenase-1 protects against ischemia and reperfusion injury in transgenic mice. *Circ Res*. 2001; 89:168–173. [PubMed: 11463724]
16. Yet SF, Perrella MA, Layne MD, Hsieh CM, Maemura K, Kobzik L, Wiesel P, Christou H, Kourembanas S, Lee ME. Hypoxia induces severe right ventricular dilatation and infarction in heme oxygenase-1 null mice. *J Clin Invest*. 1999; 103:R23–R29. [PubMed: 10207174]
17. Sodhi K, Puri N, Inoue K, Falck JR, Schwartzman ML, Abraham NG. EET agonist prevents adiposity and vascular dysfunction in rats fed a high fat diet via a decrease in Bach 1 and an increase in HO-1 levels. *Prostaglandins Other Lipid Mediat*. 2012; 98:133–142. [PubMed: 22209722]
18. Burgess A, Li M, Vanella L, Kim DH, Rezzani R, Rodella L, Sodhi K, Canestraro M, Martasek P, Peterson SJ, Kappas A, Abraham NG. Adipocyte heme oxygenase-1 induction attenuates metabolic syndrome in both male and female obese mice. *Hypertension*. 2010; 56:1124–1130. [PubMed: 21041703]
19. Nicolai A, Li M, Kim DH, Peterson SJ, Vanella L, Positano V, Gastaldelli A, Rezzani R, Rodella LF, Drummond G, Kusmic C, L'Abbate A, Kappas A, Abraham NG. Heme Oxygenase-1 Induction Remodels Adipose Tissue and Improves Insulin Sensitivity in Obesity-Induced Diabetic Rats. *Hypertension*. 2009; 53:508–515. [PubMed: 19171794]
20. Wang G, Hamid T, Keith RJ, Zhou G, Partridge CR, Xiang X, Kingery JR, Lewis RK, Li Q, Rokosh DG, Ford R, Spinale FG, Riggs DW, Srivastava S, Bhatnagar A, Bolli R, Prabhu SD. Cardioprotective and antiapoptotic effects of heme oxygenase-1 in the failing heart. *Circulation*. 2010; 121:1912–1925. [PubMed: 20404253]
21. Cao J, Vecoli C, Neglia D, Tavazzi B, Lazzarino G, Novelli M, Masiello P, Wang YT, Puri N, Paolucci N, L'Abbate A, Abraham NG. Cobalt-Protoporphyrin Improves Heart Function by

- Blunting Oxidative Stress and Restoring NO Synthase Equilibrium in an Animal Model of Experimental Diabetes. *Front Physiol.* 2012; 3:160. [PubMed: 22675305]
22. Bolognesi M, Sacerdoti D, Di PM, Angeli P, Quarta S, Sticca A, Pontisso P, Merkel C, Gatta A. Haeme oxygenase mediates hyporeactivity to phenylephrine in the mesenteric vessels of cirrhotic rats with ascites. *Gut.* 2005; 54:1630–1636. [PubMed: 16227362]
 23. Di PM, Zampieri F, Quarta S, Sacerdoti D, Merkel C, Gatta A, Bolognesi M. Heme oxygenase regulates renal arterial resistance and sodium excretion in cirrhotic rats. *J Hepatol.* 2011; 54:258–264. [PubMed: 21055838]
 24. Wang CF, Wang ZY, Li JY. Dual protective role of HO-1 in transplanted liver grafts: a review of experimental and clinical studies. *World J Gastroenterol.* 2011; 17:3101–3108. [PubMed: 21912452]
 25. Shen Z, Teng X, Qian X, He M, Hu Y, Ye W, Huang H, Yu Y, Chen Y. Immunoregulation effect by overexpression of heme oxygenase-1 on cardiac xenotransplantation. *Transplant Proc.* 2011; 43:1994–1997. [PubMed: 21693314]
 26. Besenon F, Dedja A, Vadori M, Bosio E, Seveso M, Tognato E, Polito L, Calabrese F, Valente M, Rigotti P, Ancona E, Cozzi E. In vitro and in vivo immunomodulatory effects of cobalt protoporphyrin administered in combination with immunosuppressive drugs. *Transpl Immunol.* 2010; 24:1–8. [PubMed: 20713156]
 27. Fedorova LV, Raju V, El-Okdi N, Shidyak A, Kennedy DJ, Vetteth S, Giovannucci DR, Bagrov AY, Fedorova OV, Shapiro JI, Malhotra D. The cardiotoxic steroid hormone marinobufagenin induces renal fibrosis: implication of epithelial-to-mesenchymal transition. *Am J Physiol Renal Physiol.* 2009; 296:F922–F934. [PubMed: 19176701]
 28. Cao J, Sodhi K, Inoue K, Quilley J, Rezzani R, Rodella L, Vanella L, Germinario L, Stec DE, Abraham NG, Kappas A. Lentiviral-Human Heme Oxygenase Targeting Endothelium Improved Vascular Function in Angiotensin II Animal Model of Hypertension. *Hum Gene Ther.* 2011; 22:271–282. [PubMed: 20836698]
 29. Chan EJ, Dellsperger KC. Cardiorenal Syndrome: The Clinical Cardiologists' Perspective. *Cardiorenal Med.* 2011; 1:13–22. [PubMed: 22258462]
 30. Schiffrin EL. T lymphocytes: a role in hypertension? *Curr Opin Nephrol Hypertens.* 2010; 19:181–186. [PubMed: 20040866]
 31. Geiger H. T-cells in angiotensin-II-induced vascular damage. *Nephrol Dial Transplant.* 2008; 23:1107–1108. [PubMed: 18079148]
 32. Ronco C, Cicoira M, McCullough PA. Cardiorenal syndrome type 1: pathophysiological crosstalk leading to combined heart and kidney dysfunction in the setting of acutely decompensated heart failure. *J Am Coll Cardiol.* 2012(60):1031–1042. [PubMed: 22840531]
 33. Virzi' GM, de CM, Cruz DN, Bolin C, Vescovo G, Ronco C. Type 1 cardiorenal syndrome and its possible pathophysiological mechanisms. *G Ital Nefrol.* 2012; 29:690–698. [PubMed: 23229667]
 34. Guo R, Zhou J, Deng XL, Gao GD, Jiang XY, Lin YX. Angiotensin II increases ROS production in cardiac fibroblasts by inducing p22phox over-expression. *Nan Fang Yi Ke Da Xue Xue Bao.* 2009; 29:202–204. [PubMed: 19246278]
 35. Coppo M, Boddi M, Bandinelli M, Degl'innocenti D, Ramazzotti M, Marra F, Galastri S, Abbate R, Gensini GF, Poggese L. Angiotensin II upregulates renin-angiotensin system in human isolated T lymphocytes. *Regul Pept.* 2008; 151:1–6. [PubMed: 18723052]

Novelty and Significance

1) What is New

- After MI, immunosuppressed mice have an increase in renal interlobar arterial' resistance and renal damage.
- Beneficial role of HO-1 in decreasing renal vasoconstriction and renal dysfunction is evident in T-lymphocyte suppressed mice.

2) What is Relevant?

Our data demonstrate that T-lymphocyte related immunity plays a role in the maintenance of renal morphology and vasoconstriction after post-ischemic heart failure

3) Summary

This is the first study demonstrating that T-Lymphocyte suppression allowed HO-1 dependent improvement in renal vasoconstriction and function in a model of post ischemic heart failure.

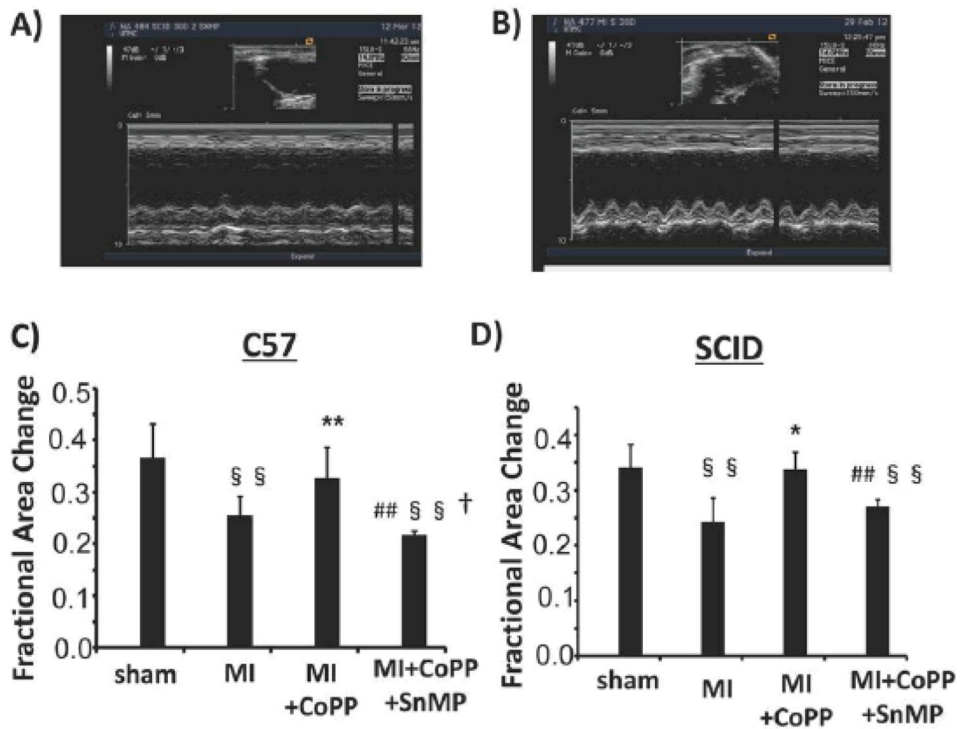


Figure 1. A) and B): M-mode images of left ventricle in a control operated (a) and MI (b) mouse. End diastolic diameter, an index of left ventricle dilatation, was augmented in MI mouse C) Fractional Area Change of C57 and SCID mice: FAC was significantly reduced after MI in both strains, CoPP treatment significantly improved EF. (§ $p < 0.05$ vs Control; § § $p < 0.01$ vs. Control; * $p < 0.05$ vs. MI; ** $p < 0.01$ vs. MI; # $p < 0.05$ vs. MI+CoPP; ## $p < 0.01$ vs. MI +CoPP; † $p < 0.05$ vs. SCID)

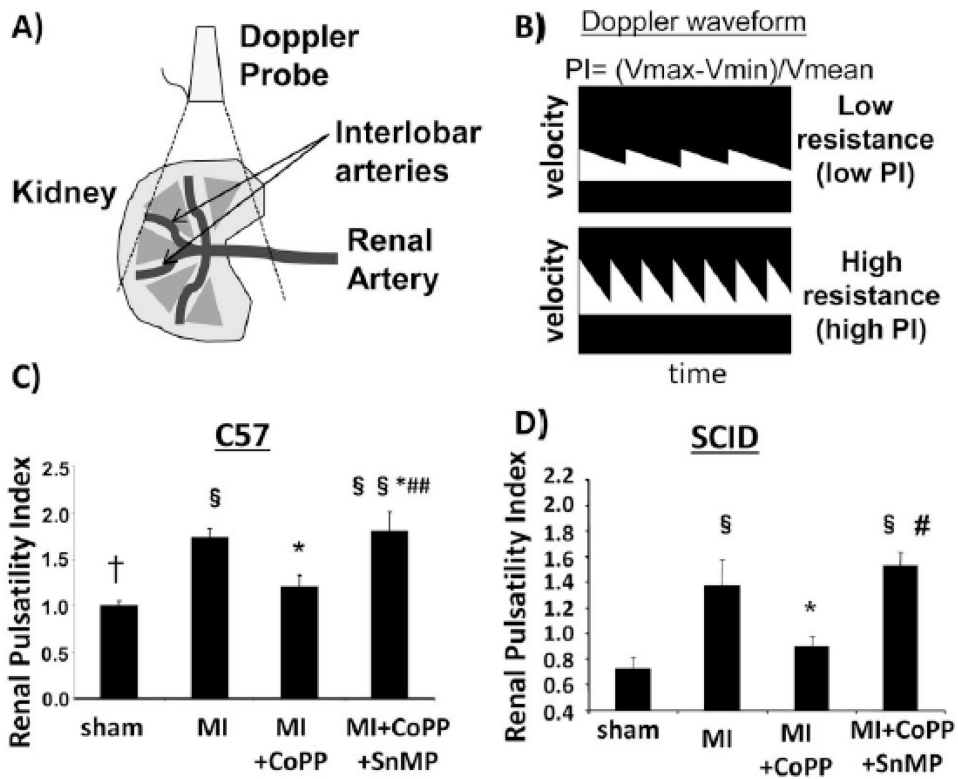


Figure 2. A) schematic representation of the kidney and the renal interlobar arteries; B) schematic representation of Doppler waveform measured in a low resistive and in a high resistance vessel; C, D) Renal Pulsatility Index of C57 and SCID mice respectively. Renal pulsatility index was used to measure renal vasoconstriction. (§ $p < 0.05$ vs Control; § § $p < 0.01$ vs Control; * $p < 0.05$ vs MI; ** $p < 0.01$ vs MI; # $p < 0.05$ vs MI+CoPP; ## $p < 0.01$ vs MI+CoPP; † $p < 0.05$ vs SCID)

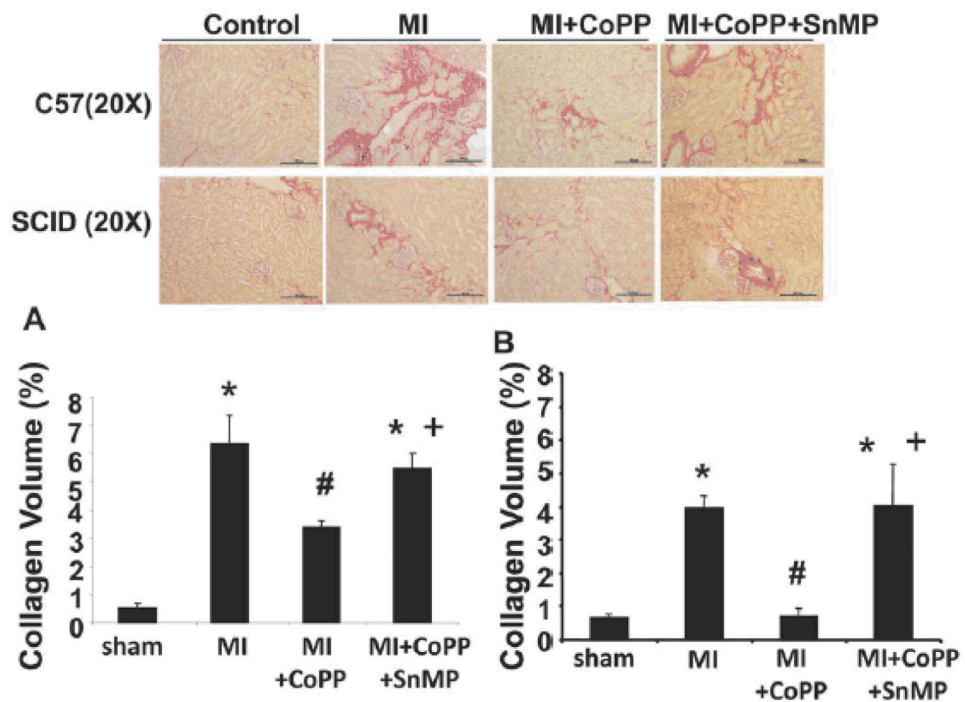


Figure 3. Effect of CoPP in C57 and SCID mice on Renal Fibrosis 30 days post MI. Results are shown as means±SE. (A, B); Sirius Red staining of interstitial collagen at the cortico-medullary junction of C57 and Scid mice kidneys respectively. Original magnification 200. Bar 100 μm. C- Computer-assisted morphometry measurements of collagen fibers content in studied groups of mice. *p<0.05 vs. Control, #p<0.05 vs. MI, +p<0.05 vs. MI+CoPP.

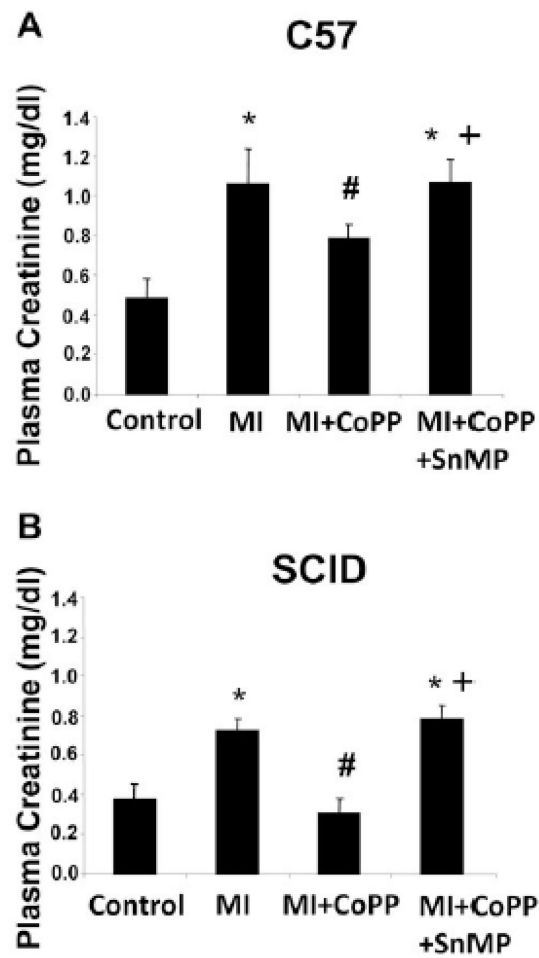


Figure 4. Effect of CoPP in C57 and SCID mice on the levels of Plasma Creatinine 30 days post MI. Results are shown as means \pm SE, (**C, D**) Plasma Creatinine level (mg/dl) of C57 and SCID mice respectively; * p <0.05 vs. Control, # p <0.05 vs. MI, + p <0.05 vs. MI+CoPP.

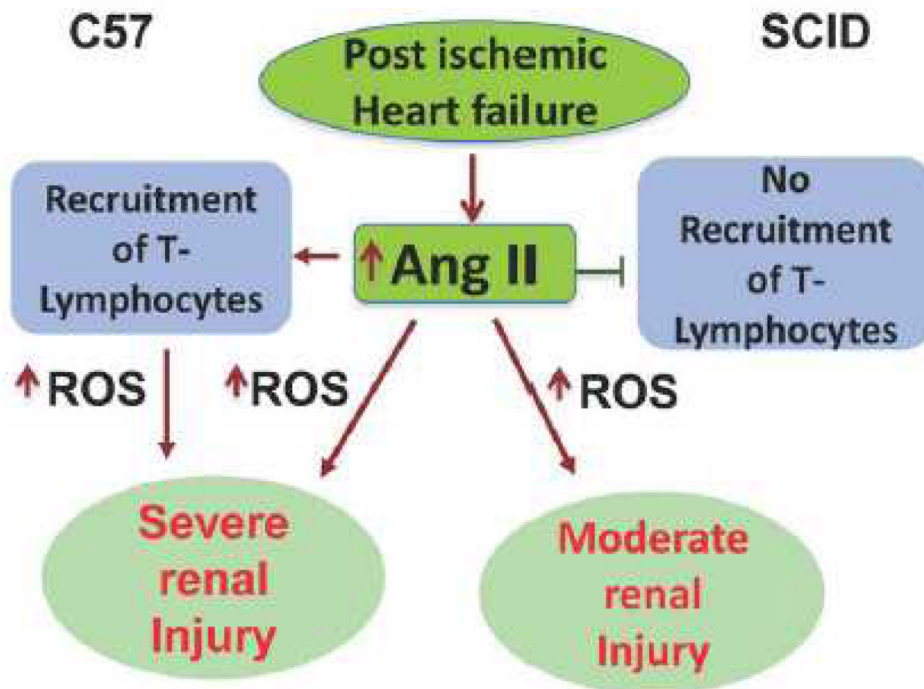


Figure 5. Proposed mechanisms showing that the decrease of the T-Lymphocyte immune response itself reduces kidney damage and renal vasoconstriction in a model of post ischemic heart failure as compared to immune-competent mice, and that suppression of T lymphocytes amplified the beneficial effects of HO-1 in improving CRS-1.

Table 1

Parameters	SHAM n _(C57,SCID) =8,7	MI n _(C57,SCID) =6,4	MI+CoPP n _(C57,SCID) =6,4	MI+CoPP+SnMP n _(C57,SCID) =5,4
Body				
<i>C57</i>	26.5±2.4	26.2±1.5	25.8±1.2	25.7±1.8
<i>SCID</i>	27.4±2.8	27.8±2.2	26±1	25±0.8
Heart				
<i>C57</i>	409±64	397±10	410±52	465±38
<i>SCID</i>	421±52	412±93	419±93	355±22
Echocardiography				
EDA(cm)	<i>C57</i> 0.154±0.02	0.216±0.02 ^{§§}	0.172±0.03 ^{**}	0.224±0.035 ^{§§#}
	<i>SCID</i> 0.15±0.02	0.18±0.02 ^{§§}	0.14±0.01 ^{**}	0.17±0.01 [#]
EDD(cm)	<i>C57</i> 0.387±0.03	0.471±0.02 ^{§§ †}	0.437±0.02 [*]	0.498±0.05 ^{§§# †}
	<i>SCID</i> 0.36±0.03	0.35±0.04 ^{§§}	0.33±0.01 ^{**}	0.39±0.03 [#]
C.I.(ml/min/Kg)				
<i>C57</i>	2034±372	1392±65 [§]	1904±307 [§]	1439±123 ^{**##}
<i>SCID</i>	2165±431	1451±43 [§]	2037±227 ^{§§}	1560±193 ^{§§*}
Renal EchoDoppler				
PI	<i>C57</i> 0.95±0.005 [†]	1.16±0.096 [§]	1.14±0.092 [§]	1.89±0.23 ^{§#}
	<i>SCID</i> 0.72 ±0.08	1.38±0.20 [§]	0.90±0.19 [*]	1.53±0.1 [§]

C57 and SCID mice: in vivo heart measurements by echocardiography and renal echo. Doppler 30 days after MI. Values are expressed as mean ± SD; n= number of animals tested; EDA= end diastolic area, EDD= end diastolic diameter; PI= pulsatility index;

* p<0.05 vs MI;

** p<0.01 vs MI;

§ p<0.05 and

§§ p<0.01 vs sham;

p<0.05 vs MI+CoPP;

p<0.01 vs MI+CoPP;

† p<0.05 vs SCID.